Utilizing Solar Infrared-induced Photothermal Heating on Building Windows in Winter

Enhe Zhang, Qiuhua Duan, Yuan Zhao, Julian Wang*

Department of Architectural Engineering

104 Engineering Unit A

The Pennsylvania State University

University Park, PA 16802

*** Corresponding author：** Julian Wang, julian.wang@psu.edu

Abstract

Single-pane windows still account for a large percentage of the US building energy consumption. In this paper, we introduced a new solution incorporating the photothermal effect of metallic nanoparticles (Fe_3O_4@Cu_{2-xS}) into glazing structures to utilize solar infrared and then enhance the window's thermal performance in winter. Such spectrally selective characteristics of the designed photothermal films were obtained from lab measurements and then integrated into a thermodynamic analytical model. Subsequently, we examined the thermal and optical behaviors of the photothermal single-pane window and compared its overall energy performance with the conventional low-e coated single-pane window, in which typical window properties, dimensions, winter boundary conditions, and solar irradiance were adopted. The numerical analysis results demonstrated that the photothermal window systems could yield 20.4% energy savings relative to the conventional low-e coated windows. This research paves an underlying thermodynamic mechanism for understanding such a nanoscale phenomenon at the architectural scale. From the implementation perspective, the designed photothermal film can be added into the existing single-pane windows for energy-efficient retrofitting purposes.

Keywords: Building windows, Solar radiation, Photothermal effect, Energy savings, Optical behaviors, Thermodynamics.

1. Introduction

It was reported that the buildings are responsible for 41% of primary energy consumption in the United States.[1] The physical properties of building envelopes may have an impact on building energy consumption. In general, 30 ~40% of current building windows are single-pane, even in northern areas in the USA, and they are responsible for over 50% of the total energy loss in the United States.[2] To improve the performance of building windows, adding low emissivity (low-e) coating on existing windowpanes is one of the main practical strategies. The low-e coating is a micro-thin layer of thermally reflective materials that can be applied to the surface of the glass. The low-e coated windows can not only reduce radiative heat transfer by reflecting solar radiation to the exterior in summer but also lower heating needs in winter by keeping the heat from radiating to the outside. Consequently, adding low-e coatings or window films may decrease HVAC energy consumption so that they have been commonly recommended to retrofit existing building windows.[3] However, Wang and Shi demonstrated that it had been a great challenge to achieve coincident high solar-infrared transmittance and low emissivity in longwave radiation.[4] As such, even the high solar heat gain coefficient (SHGC) low-e coating (e.g., single silver unit) may reflect about 50% solar near-infrared (NIR) to outdoor, which may offset the solar heat gain benefits for indoor heating energy savings in winter.

Selection and/or peer review under responsibility of Scientific Committee
doi:10.18086/solar.2020.01.04 Available at http://proceedings.ises.org

In this research, we introduced and then analytically examined a new spectrally selective nanostructure, based on metallic nanoparticles' photothermal effect discovered in recent years, that can be added on the existing low-e window systems and utilize the solar NIR for heating energy saving purposes in winter.

2. Photothermal effects and heating experiments under simulated solar light

The photothermal (PT) effect has been investigated for biomedical applications in the past two decades, such as the studies on sensing, imaging, therapies, and drug deliveries.[5,6] The PT effect includes two stages, the photonic energy absorption, and photon-induced heat generation. The first stage usually happens in the way of absorption and may exist in other photonic extinction due to the microstructure of the material, such as multiple scattering. The second stage is the conversion of absorbed light energy to thermal energy. For metal or some semiconductor nanoparticles, Localized Surface Plasmon Resonance (LSPR) is believed to be the main reason for their photothermal effect.[7] As

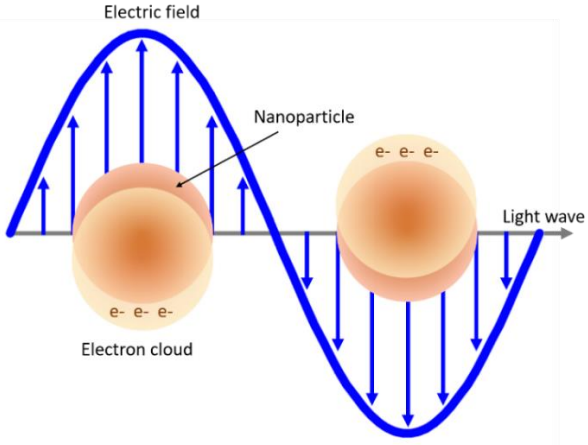

Figure 1. Schematic diagram of LSPR.

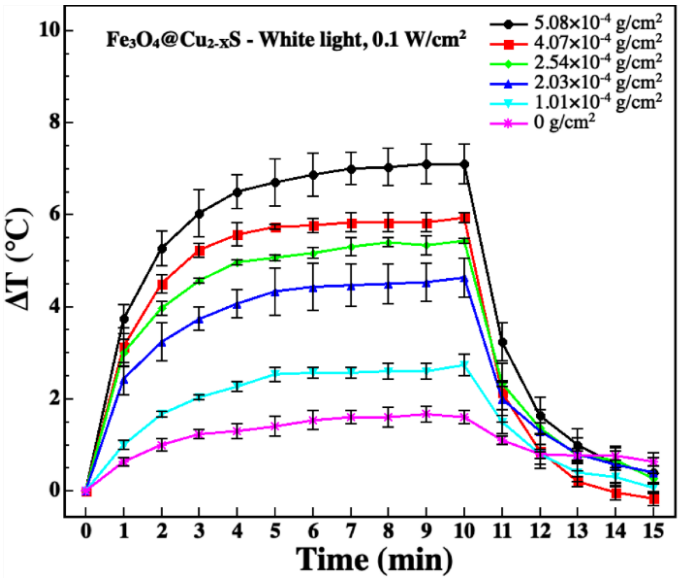

Figure 2. Temperature Change diagram.

shown in Figure 1, LSPR is driven by photoexcitation when the incident frequency matches the natural frequency of the oscillating surface electrons. This excitation causes an inhomogeneity in the electron density of a conductor,

generating a local electrical field that tends to drive charge equilibration. Electrons accelerating through this field can pick up enough energy to overshoot equilibrium configuration and effectively switch the local electric field, causing an oscillation. This oscillation is not perpetual, thus requiring photoexcitation for maintenance. More importantly, various research efforts have been focused on manipulating the absorptions into the desired regions, which provides strong potential in solar infrared modulation for building applications. While controlling transmitted solar infrared thermal radiation, an ideal window should be capable of sufficient transmission of visible light, which is associated with the window's optical property of visual transmittance (VT). A higher VT brings more daylight to the interior and may offset electric lighting, especially for spaces with a great lighting demand. It has been reported that window's VT ranges from above 90% to less than 10%, determined by glazing type, number of panes, and glass coatings or films.[8] Solar NIR-induced photothermal effect may independently modulate the solar heat without (or with slight) compensation of the visible transmittance. However, before incorporating such photothermal effect into building windows, it is necessary to perform an in-depth energy-saving analysis to understand its energy impacts and associated thermal and optical behaviors.

Note that the energy-saving analysis of this study was based on experimental results in our previous report.[9] Specifically, Fe_3O_4@Cu2−xS nanoparticles were synthesized and coated on glass substrates (2.54 × 2.54 cm^2). Samples are made in specific average visible transmittance (AVT): 65%, 70%, 75%, 80% and 85%. The coated samples were irradiated by 0.1 Wcm^{-2} simulated solar light by a Newport 150W solar simulator, as shown in Figure 2. The temperature was monitored by a FLIR E6 infrared camera. In particular, FC-75% achieved a 5.43 °C temperature increase, which was then utilized in the following analytical analysis.

3. Energy-saving analysis of photothermal single-pane windows

Solar radiation interaction with the earth atmosphere results in four solar components: direct normal irradiance (DNI), diffuse horizontal irradiance (DHI), global horizontal irradiance (GHI), and reflected ground radiation (Rg).[10] For vertical windows of a building, the average global radiation can be estimated by Liu-Jordan isotropic model.[11] Solar radiation on windows is either transmitted, absorbed, or reflected in varying amounts depending on the wavelength. Solar heat gains through a window system can be determined from the overall transmittance and the absorptance of each pane or layer as a function of the angle of incidence. The transmitted solar radiation may directly reduce indoor heating energy use. In contrast, the absorbed solar radiation may partially flow inward from the panes to indoor, which may also increase the temperature of indoor, and consequently improve heating energy savings in winter. In brief, compared with the low-e coated windows, the addition of photothermal coatings may slightly reduce the transmitted amount of solar radiation but theoretically lead to a significant increase of the inward flowing heat due to the photothermal effects through absorbing the solar radiation. In this work, we firstly used OPTICS of the WINDOW program to build the low-e coated single-pane window (as the baseline or called Type 1) and the photothermal window (Type 2). Then we output the spectral characteristics of the two types of window models developed. Combing the spectral properties derived and the calculated incident solar radiation, we then calculated the transmitted and absorbed solar radiation. Subsequently, the PT effect yielded in our previous material experiments was successfully incorporated into thermodynamic analyses and calculations of the inward flowing thermal radiation. This computation was completed by using a thermal transfer analytical model built in Matlab. Finally, we compared the net energy based on the heating loads in terms of transmitted solar gains and inward flowing thermal radiation, of the two types of windows.

3.1 Incident solar irradiance on vertical window surfaces

The total ("global") hemispherical radiation on a plane, G or GHI, is defined as Equation (1). It is the combination of the direct normal radiation multiplied by the cosine of the incidence angle θ (between the normal to the plane and the

direction from the base of the normal to the center of the solar disk), DNI cos(θ) or B cos(θ), plus the diffuse sky radiation DHI or D.[12]

$$G = \mathrm{B}\cos(\theta) + \mathrm{D} \qquad \text{(eq. 1)}$$

For a titled plane with titled angle β, diffuse irradiance D is defined as Equation (2) by using Liu-Jordan isotropic model.[11] Meanwhile, the global (total) hemispherical irradiance on the tilted plane should consider the reflected ground radiation Rg so that G can be obtained by Equation (3).

$$\mathrm{D} = D_h * 0.5 * (1 + \cos\beta) \qquad \text{(eq. 2)}$$

Where, D_h is diffused horizontal irradiance.

$$G = \mathrm{B}\cos(\theta) + \mathrm{D} + R_g\beta) \qquad \text{(eq. 3)}$$

$$R_g = \rho \cdot G_h \cdot R_h\beta) \qquad \text{(eq. 4)}$$

Where, ρ is foreground's albedo, G_h is global horizontal irradiance, R_h is the ground reflected horizontal irradiance $R_h = 0.5 \cdot (1 - \cos\beta)$, β is a tilted angle.

We selected solar spectra data collected by using ASTM G173-03 Reference Spectra Derived from SMARTS v. 2.9.2,[13] and considered a vertical window façade facing south in State College, Pennsylvania at noon on December 21st, 2019, the incident angle for solar θ is 26°, the titled angle for vertical windows β is 90°. We obtained the incident global solar irradiance G = 636 W/m^2 on the vertical window surface, and the solar irradiation curve on the vertical plane is shown in Figure 3. Please note that this simplified method of calculating incident solar irradiance on the vertical surface may overlook the effect of ground reflection and the complexity of sky conditions. However, this would not significantly affect our next comparisons between the two types of windows as long as the same solar irradiance data for those two windows were utilized.

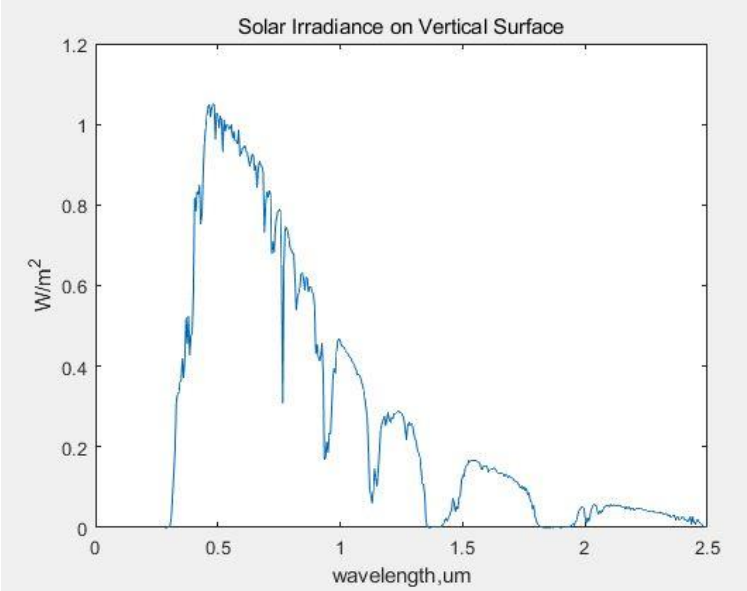

Figure 3. Solar Irradiation Curve.

3.2 Window modeling and spectral properties

We designed two types of single-pane glazing in OPTICS software, which was developed by the Lawrence Berkeley National Laboratory (LBNL). Type 1 was low-e coating single-pane glazing, which was made up of clear glass (NFRC

ID 8203) and low-e coating (NFRC ID 1511). Type 2 was the photothermal low-e single-pane glazing, which consisted of Type 1 plus a photothermal film. The photothermal film was the above-mentioned FC-75% Fe3O4@Cu2−xS film, and its spectral data measured in the lab was loaded manually in OPTICS. An import data can be customized by several key parameters, including transmittance, reflection front, reflection back, thickness, conductivity, and emissivity. The photothermal film layer was placed on the external surface of the low-e coated glass. Figure 4 illustrates the structures of Type 1 and Type 2, and Figure 5 displays their spectral properties (spectral transmission curve and absorptive curve).

As shown in Figure 5, Type 2 window had a 45.1% higher absorption (α), and it absorbed more solar radiation, mainly focusing on the solar NIR band. As a tradeoff, it has a 6.6% lower visible transmittance (τ), which allowed slightly less solar radiation to be transmitted through the window. Furthermore, the window properties, including solar heat SHGC, VT, U-factor, and solar transmittance (Ts) were obtained using OPTICS and WINDOW, as shown in Table 1. The results indicate a similar property performance, and the comparison for each parameter needs to be done before we can move on to the capability of temperature increasing. Type 1 and Type 2 have the same U-factor that is related to the thermal resistance of each layer of the window structure, which can be explained by the fact that the thin layer coating added did not have much influence on the thermal resistance. Type 2 has a slightly lower visible transmittance than the value of Type 1, which also influences SHGC. By simply calculation of the transmitted solar gains using the above solar transmittance calculated from the WINDOW OPTICS, we found that Type 1 window transmitted 335.95 W m^{-2}, while Type 2 window transmitted 323.01 W m^{-2}. In other words, the addition of the PT coating reduced 12.94 W m^{-2} solar gains to the interior.

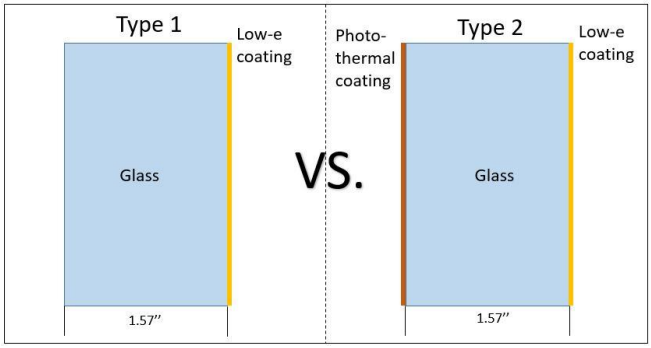

Figure 4. Window System Diagram in Optics software.

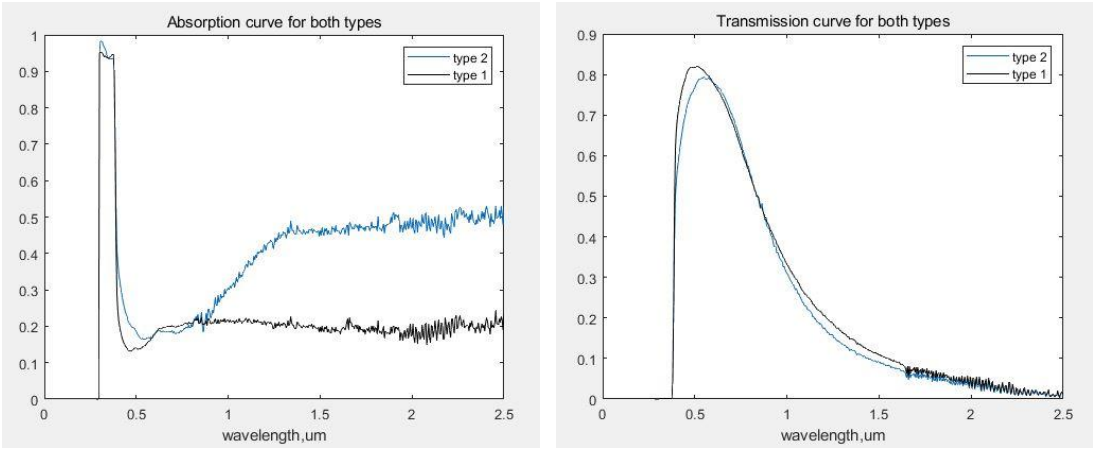

Figure 5. a) Absorption curves for both types in Optics. b) Transmission curves for both types in Optics.

In summary, the differences in the visible and full spectral transmittances of solar radiation in both types of windows were very minimal, which were about 2.1% and 3.6%, respectively. The significant difference is in the solar NIR band that was absorbed by Type 2 but reflected by Type 1.

Table 1. Window optical Properties.

	U factor, W m^{-2} K^{-1}	SHGC	Tvis	Ts
LowE+glass, type 1	3.496	0.537	0.799	0.504
LowE+glass+PT, type 2	3.496	0.533	0.782	0.486

3.3 Analytical studies for thermal behaviors

Without solar radiation involvements, the thermodynamic analysis is quite straight forward, which can be completed based on the given indoor and outdoor boundary conditions and glazing properties. However, in this study, due to the existence of solar irradiance, non-negligible absorbed solar energy, and incorporation of the photothermal effect, more comprehensive thermodynamic analytical models were needed.

First, the transmitted solar radiation, Q_{trans}, could be simply calculated by Equations (3) and (5) with the given glazing area. Similarly, the solar radiation absorbed Q_{abs} by the glazing system could be obtained by Equations (3) and (6), which might increase the glazing system's temperature, especially for the photothermal windows (Type 2).[14]

$$q_{trans} = G_h * \tau \qquad \text{(eq. 5)}$$

$$q_{abs} = G_h * \alpha \qquad \text{(eq. 6)}$$

The thermal energy-driven temperature change could be expressed as Equation (7) based on the specific heat capacity formulas: [15]

$$Q_{mal} = \int_t^{t+1} c * m * \Delta T * dt \qquad \text{(eq. 7)}$$

Where heat capacity *c* is in a unit of J gm^{-1} K^{-1}, m is the material mass in gm, ΔT is the temperature change for the material in a time-period *t*, indicated as $(T_{t+1}-T_t)$.

Second, under-designed internal and external boundary conditions, all three (conductive, convective, and radiative) types of heat transfer were calculated. In this case, with negligible forced convection, the convection and conduction were referred to buoyancy force called free convection flows.[16] The governing equations involved in Nusselt number, Prandtl number, Grashof number, and Reynolds number that were related to the thermal conductivity of air to the temperature changes. The convection and conduction occurred among the surrounding air; the assumption was that the window materials are isothermal. The conductivity of air is related to the temperature shown in the following equations.

For external free convection flows (vertical plate) could be obtained in Equations (8), (9), and (10): [17]

$$Nu_L = 0.68 + \frac{0.670 * Ra_L^{1/4}}{[1 + (0.492/Pr)^{9/16}]^{4/9}}, Ra_L \leq 10^9 \qquad \text{(eq. 8)}$$

Ra_L is the Rayleigh number calculated in Equation (9), Nu is the Nusselt number, [16]

$$Ra_L = GR_L * \Pr = \frac{g * \beta * (T_s - T_\infty) * L^3}{\upsilon * \alpha} \qquad \text{(eq. 9)}$$

In the function above, g is the gravity on earth, L is the height of the window surface, β is expansion coefficient =1/Tf, Tf is the absolute temperature $= (T_s + T_\infty)/2$, T_s is the glass surface temperature including both surfaces $T_{in,s}$ and $T_{out,s}$, T_∞ is the ambient temperature including both inner and outer $T_{in,\infty}$ and $T_{out,\infty}$. υ is the kinematic viscosity =μ/ρ, α is thermal diffusivity=k/(ρ*Cp),[18] where μ, k, Cp, ρ, and Pr are dynamic viscosity, thermal

conductivity, specific heat, density, and Prandtl number factors related to the surface air temperature(100 K to 3000 K).[19] Free convection from the panel to the surroundings is given by Newton's Law of cooling as well as conduction and radiation are shown in Equation (10), (11) and (12), respectively.[16]

$$Q_{conv} = \mathrm{h}A_s(T_s - T_\infty) \quad \text{(eq. 10)}$$

Where h=$Nu_L * k/L'$, A_s is the area of the glass surface. L'=A/P.

The net rate of radiation heat transfer between the glass and the surroundings is,

$$Q_{rad} = \varepsilon\sigma A_s(T_s - T_\infty) \quad \text{(eq. 11)}$$

ε is the emissivity, σ is Stefan–Boltzmann constant 5.67E-08 W m^{-1} K^{-1}.

$$Q_{cond} = \mathrm{k}A_s(T_s - T_\infty)/L' \quad \text{(eq. 12)}$$

L' is the thickness of the glass. But use the same assumption as conduction

Third, based on equations (6), (7), (10), (11), and (12), the thermal balance model can be written as in two equations (13) and (14):

$$Q_{abs} = Q_{conv} + Q_{cond} + Q_{rad} + \mathrm{Q}_{mal} * t \quad \text{(eq. 13)}$$

$$Q_{abs} = q_{abs} * A_s \quad \text{(eq. 14)}$$

In the comparison of Type 1 and Type 2, they all placed under the same solar irradiation conditions, which were based on the reference solar spectra. The outdoor temperature was 0 °C, and the indoor temperature remained 25 °C. The dimension of this glazing system was 1.2m by 1.5m. Besides, the surrounding relative humidity was set as a constant 50% RH. Also, in this comparison, we ignored other effects by window frames, glazing edges, condensation risks, etc.

By using the above governing functions, we then derived the window surface temperatures and the inward flowing thermal radiation values. As shown in Table 2, the total solar absorption Q_{abs} are 183.83 W m^{-2} and 139.38 W m^{-2} for Type 1 and Type 2, respectively. Type 2 gained 44.45 W m^{-2} more than Type 1 on absorption. Affected by the PT effect, that difference resulted in a 23.84 K temperature increase for the inner window surface temperature of Type 2, compared with that temperature of Type 1, as shown in Table 2. The temperature difference between the window's inner surface temperature and interior ambient temperature formed thermal transfer that could be calculated using Equations (10), (11), and (12). As shown in the results Table 2, the heat transfer to the indoor area through convection, conduction, and radiation were -10.19 and 69.18 W m^{-2} for Type 1 and Type 2, respectively. The negative sign of heat transfer represents a heat loss from the indoor area to outside. It also indicated that the PT effect significantly increased the inner surface temperature and even became a thermal radiation source for the interior.

Table 2. Window thermal properties.

In winter	Q_{abs}, W m^{-2}	Q_{trans}, W m^{-2}	Material T, K	$T_{in,s}$ / $T_{out,s}$, K		Heat transfer to indoor, W m-2
Type 1	139.38	335.95	294.08	294.29	293.86	-10.19
Type 2	183.83	323.01	317.92	318.14	317.71	69.18

3.4 Heating energy saving analysis

Combining the results from the above sections 3.2 and 3.3, we were able to calculate the net energy based on the solar heat gains and the building heat loss through windows: 325.76 W m^{-2} for Type 1, and 392.19 W m^{-2} for Type 2. The

net energy amounts are shown in Table 2: 325.76 W m^{-2} and 392.19 W m^{-2} for Type 1 and Type 2, respectively. In short, this represents that the photothermal window (Type 2) could achieve 20.4% energy savings than the baseline window (Type 1) in winter and with solar radiation situations.

4. Conclusion

In this paper, we proposed a solution of using a photothermal thin film to enhance the thermal performance of low-e coated single-pane windows. Then, we focused on the development of a comprehensive thermodynamic analytical model into which we incorporated the photothermal effect. Through this analytical model and computation, we concluded that compared with the low-e coated windows, 20.4% energy-savings could be yielded by the photothermal windows in winter. Notably, this energy-saving was not achieved by increasing the thermal insulation but rather by the spectrally selective design of glazing materials and utilization of solar NIR. Our future works include three trajectories. First, further work of this model is looking to bring more flexible inputs such as the variability of ambient temperature into the models. Also, the wind speed was negligible in the model to avoid forced convection calculations in this study. Second, we plan to apply hourly weather data, including the solar NIR value, and then predict annual energy savings. We will incorporate our previous study of solar NIR modeling into this annual energy analysis.[20] Last, in addition to the energy savings due to the PT effect, the PT effect may also reduce the risks of window condensation by increasing the temperature of the window's inner surface. The condensation occurred on building windows, especially low-e coated single-pane windows, which may lead to significant thermal loss from indoor to outdoor. [21] Therefore, the combined energy savings on window condensation improvements and enhanced solar heat gains need to be investigated with more thorough and dynamic energy analysis methods.

6.Acknowledgements

We acknowledge the financial supports provided by the National Science Foundation CMMI-1847024 and National Science Foundation CMMI-1953004.

References:

1. Zimmer A, Ha. H. Buildings and Infrastructure from a Sustainability Perspective. *Sustain Heal Communities Program-Theme 41*. 2014;1:2016-09.
2. Carmody J, Selkowitz S, Lee eleanor s., Arashteh D, Willmert T. Window System for High-Performance Buildings. *WW Norton&Company*. 2004.
3. LOW-EMISSIVITY WINDOW FILM. https://www.gsa.gov/cdnstatic/GPG_Findings_032-Low-E_Film.pdf. Accessed July 12, 2020.
4. Wang J (Jialiang), Shi D. Spectral selective and photothermal nano structured thin films for energy efficient windows. *Appl Energy*. 2017;208:83-96. doi:10.1016/j.apenergy.2017.10.066
5. Kim M, Lee JH, Nam JM. Plasmonic Photothermal Nanoparticles for Biomedical Applications. *Adv Sci*. 2019. doi:10.1002/advs.201900471
6. Zhao Z, Yuan J, Zhao X, Bandla A, Thakor N V., Tan MC. Engineering the Infrared Luminescence and Photothermal Properties of Double-Shelled Rare-Earth-Doped Nanoparticles for Biomedical Applications. *ACS Biomater Sci Eng*. 2019. doi:10.1021/acsbiomaterials.9b00526
7. Link S, El-Sayed MA. Shape and size dependence of radiative, non-radiative and photothermal properties of gold nanocrystals. *Int Rev Phys Chem*. 2000. doi:10.1080/01442350050034180
8. Wang J, Caldas L, Chakraborty D, Huo L. Selection of energy efficient windows for hot climates using genetic algorithms optimization. In: *Cities, Buildings, People: Towards Regenerative*

Environments. In Proceedings of PLEA 2016, International Conference on Passive and Low Energy Architecture 2016; 2016:11-13.

9. Lin J, Zhao Y, Shi D. Optical thermal insulation via the photothermal effects of Fe3O4 and Fe3O4@Cu2-xS thin films for energy-efficient single-pane windows. *MRS Commun*. 2020. doi:10.1557/mrc.2020.4
10. Myers DR. *Solar Radiation: Practical Modeling for Renewable Energy Applications*.; 2017. doi:10.1201/b13898
11. Liu BYH, Jordan RC. The long-term average performance of flat-plate solar-energy collectors. With design data for the U.S., its outlying possessions and Canada. *Sol Energy*. 1963. doi:10.1016/0038-092X(63)90006-9
12. NREL. Global Horizontal Radiation. https://www.nrel.gov/grid/solar-resource/solar-glossary.html.
13. NREL. *Air Mass 1.5: ASTM G-173-03*. https://www.nrel.gov/grid/solar-resource/spectra.html.
14. Marion W, Wilcox S. *Solar Radiation Data Manual For Buildings*. Golden Colorado https://www.nrel.gov/docs/legosti/old/7904.pdf.
15. Reif F, Scott HL. Fundamentals of Statistical and Thermal Physics. *Am J Phys*. 1998. doi:10.1119/1.19073
16. Incropera FP, De Witt DP. Fundamentals of heat transfer. 1981. doi:10.13182/nse65-a18809
17. Spalding DB. Handbook of heat transfer. *Int J Heat Mass Transf*. 1975. doi:10.1016/0017-9310(75)90148-9
18. Bird RB, Stewai WE, Lightfoot. EN. *Phenomena Second Edition.* academia.edu
19. Zografos AI, Martin WA, Sunderland JE. Equations of properties as a function of temperature for seven fluids. *Comput Methods Appl Mech Eng*. 1987. doi:10.1016/0045-7825(87)90003-X
20. Duan Q, Feng Y, Zhang E, Song Y, Wang J, Niu S. Solar Infrared Radiation towards Building Energy Efficiency: Measurement, Data, and Modeling. *Environ Rev*. 2020.
21. Duan Q, Zhao Y, Wang. J. Thermal performance and condensation risk of single-pane glazing with low emissivity coatings. *MRS Adv*. 2020:1-10.